(4)

TECHNICAL REPORT ARCCB-TR-89008

WAVE COUPLING AND

RESONANCE IN GUN TUBES

AD-A207 098

T. E. SIMKINS

DTIC
S ELECTE D
D APR2 1 1989

MARCH 1989

US ARMY ARMAMENT RESEARCH,
DEVELOPMENT AND ENGINEERING CENTER
CLOSE COMBAT ARMAMENTS CENTER
BENÉT LABORATORIES
WATERVLIET, N.Y. 12189-4050

APPROVED FOR PUBLIC RELEASE; DISTRIBUTION UNLIMITED

089 4 21 076

DISCLAIMER

The findings in this report are not to be construed as an official Department of the Army position unless so designated by other authorized documents.

The use of trade name(s) and/or manufacturer(s) does not constitute an official indorsement or approval.

DESTRUCTION NOTICE

For classified documents, follow the procedures in DoD 5200.22-M, Industrial Security Manual, Section II-19 or DoD 5200.1-R, Information Security Program Regulation, Chapter IX.

For unclassified, limited documents, destroy by any method that will prevent disclosure of contents or reconstruction of the document.

For unclassified, unlimited documents, destroy when the report is no longer needed. Do not return it to the originator.

3 May 1989

ERRATA SHEET
(Change Notice)

C1 TO: TECHNICAL REPORT ARCCB-TR-89008

WAVE COUPLING AND RESONANCE IN GUN TUBES

by

T. E. Simkins

Please remove pages i and 17 and 18 from
above Technical Report and insert new pages
enclosed. The caption for Figure 8b has
been changed.

US ARMY ARMAMENT RESEARCH, DEVELOPMENT,
AND ENGINEERING CENTER

CLOSE COMBAT ARMAMENTS CENTER

BENET LABORATORIES

WATERVLIET, N.Y. 12189-4050

REPORT DOCUMENTATION PAGE		READ INSTRUCTIONS BEFORE COMPLETING FORM
1. REPORT NUMBER ARCCB-TR-89008	**2. GOVT ACCESSION NO.**	**3. RECIPIENT'S CATALOG NUMBER**
4. TITLE (and Subtitle) WAVE COUPLING AND RESONANCE IN GUN TUBES		**5. TYPE OF REPORT & PERIOD COVERED** Final
		6. PERFORMING ORG. REPORT NUMBER
7. AUTHOR(s) T. E. Simkins		**8. CONTRACT OR GRANT NUMBER(s)**
9. PERFORMING ORGANIZATION NAME AND ADDRESS U.S. Army ARDEC Benet Laboratories, SMCAR-CCB-TL Watervliet, NY 12189-4050		**10. PROGRAM ELEMENT, PROJECT, TASK AREA & WORK UNIT NUMBERS** AMCMS No. 6111.02.H610.011 PRON No. 1A84Z8CANMSC
11. CONTROLLING OFFICE NAME AND ADDRESS U.S. Army ARDEC Close Combat Armaments Center Picatinny Arsenal, NJ 07801-5000		**12. REPORT DATE** March 1989
		13. NUMBER OF PAGES 21
14. MONITORING AGENCY NAME & ADDRESS(if different from Controlling Office)		**15. SECURITY CLASS. (of this report)** UNCLASSIFIED
		15a. DECLASSIFICATION/DOWNGRADING SCHEDULE

16. DISTRIBUTION STATEMENT (of this Report)

Approved for public release; distribution unlimited.

17. DISTRIBUTION STATEMENT (of the abstract entered in Block 20, if different from Report)

18. SUPPLEMENTARY NOTES

Presented at the Fifty-Ninth Shock and Vibration Symposium,
Albuquerque, NM, 18-20 October 1988.
Published in Proceedings of the Symposium.

19. KEY WORDS (Continue on reverse side if necessary and identify by block number)

Wave Motion in Solids
Vibrations
Resonance
Flexure

20. ABSTRACT (Continue on reverse side if necessary and identify by block number)

Uncommonly large dynamic strains observed during the firing of a 120-mm gun tube
have been found to be due to a projectile velocity which causes resonant type
behavior of a particular axisymmetric wave. The theory explaining this
phenomenon is reviewed and extended to show the potential for excitation of non-
axially symmetric waves through coupling when the tube has an eccentric bore.
These non-axially symmetric waves, one of which resonates at a projectile
velocity extremely close to that which causes axisymmetric resonance, cause a
beamlike motion of the gun tube which can affect accuracy at the target.

TABLE OF CONTENTS

LIST OF ILLUSTRATIONS

INTRODUCTION

The work presented herein was motivated by a collection of unusual strain data acquired during a series of test firings of a 120-mm gun tube during the latter part of 1985. During these tests, circumferential strains exceeding three times those predicted by the customary Lamé design formula (ref 1) were recorded from the outer surface of this tube a few feet from the muzzle. Subsequent inspection of the strain data showed that these strains increased dramatically with projectile velocity and possessed an oscillatory waveform with a frequency approaching 15 kHz.

It was soon discovered that the extremely large strains were caused by a projectile velocity which was very close to critical. The existence of such a critical velocity had been predicted in the literature at least thirty years ago (refs 2-4), but to the best of our knowledge, no observations such as these have been reported in the literature. In the following, the essence of the 'critical velocity' theory of axisymmetric vibrations of a circular cylinder is reviewed and the theory is extended to include the case of non-axially symmetric vibrations which can be excited through coupling.

CRITICAL VELOCITY THEORY

This theory predicts a limit as to how fast the tube deformation--in the immediate vicinity of the projectile--can be made to travel before some sort of wave develops. An exaggerated view of this deformation when the projectile velocity is low is shown in Figure 1. Under these 'quasi-static' conditions, the deviation from the Lamé-predicted deformation is less than 3 percent. However, as the projectile velocity approaches a certain critical value, the tube deformation in the neighborhood of the base of the projectile--that is, at

---

References are listed at the end of this report.

1

the front of the moving pressure--grows dramatically. As with classical reso-
nance, the deformation is theoretically unbounded when the critical velocity is
reached unless damping is present.
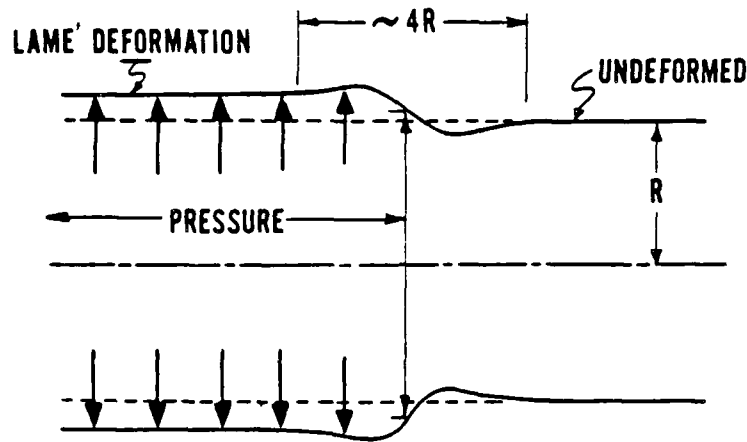
DEFORMATION OF BORE SURFACE
(STATIC)

Figure 1

The simplest equation containing the essential physics of the situation is
(ref 2)

$$D \frac{\partial^4 w}{\partial x^4} + \frac{Eh}{R^2} w + m \frac{\partial^2 w}{\partial t^2} = Q(1-H(x-vt)) \qquad (1)$$

where Q is a constant and represents the magnitude of the pressure which is
assumed to be moving at constant velocity v. H is the heaviside step function

$$H(x-vt) = 0 \quad x < vt$$
$$= 1 \quad x > vt$$

In this equation, w is the radial displacement of a point on the median surface
of a cylindrical shell located at a distance x along, and R from, the central
axis; h is the shell thickness and is assumed to be small compared to R; $m = \rho h$
where ρ is the mass density of the shell material; $D = Eh^3/12(1-\nu^2)$; E is

2

Young's modulus of elasticity; ν is Poisson's ratio; and v is the velocity of the moving pressure, assumed to be finite and constant.

Conventionally, steady-state solutions to Eq. (1) are sought under the conditions that the displacement remain bounded at $x = \pm \infty$ and that the stresses and displacements be continuous at the location of the pressure front $x = vt$. Usually, a change of variable from x to ξ is made where $\xi = x-vt$. Then the moving pressure front (the projectile) is always at $\xi = 0$ and the partial differential equation (Eq. (1)) becomes an ordinary differential equation which is easily solved. In particular, these solutions have the form $w = Ae^{\pm ik\xi}$ and are steady when seen by an observer moving with the pressure front at $\xi = 0$. k is the wave number and, in general, is complex. Only when k is real does the assumed form of the solution represent a wave. To find what waves can exist naturally in the cylinder, one sets $Q = 0$, and substitutes the assumed solution into Eq. (1). It is seen that real waves are possible for those values of k which are the real roots of the equation

$$v(k) = k\sqrt{\frac{D}{m}\left(1+\left(\frac{\gamma}{k}\right)^4\right)} \qquad (2)$$

where $\gamma^4 = \frac{Eh}{R^2 D}$ and v is the phase velocity (real). A plot of these wave numbers versus phase velocity is called a dispersion curve and is shown in Figure 2 ($C_c = \sqrt{E/\rho}$). This plot shows that waves with low wave number (long waves) travel with phase velocities which decrease with wave number, while those with high wave number (short waves) have phase velocities which increase with wave number. This happens because of two competing restoring forces in Eq. (1). The tube can deform as a cylindrical membrane in which case the second term of Eq. (1) dominates the behavior, or the tube wall can undergo axisymmetric flexure in which case the first term dominates. The fact that these two restoring forces

compete to produce a minimum in the dispersion curve of Figure 2 is the important part of the critical velocity theory.
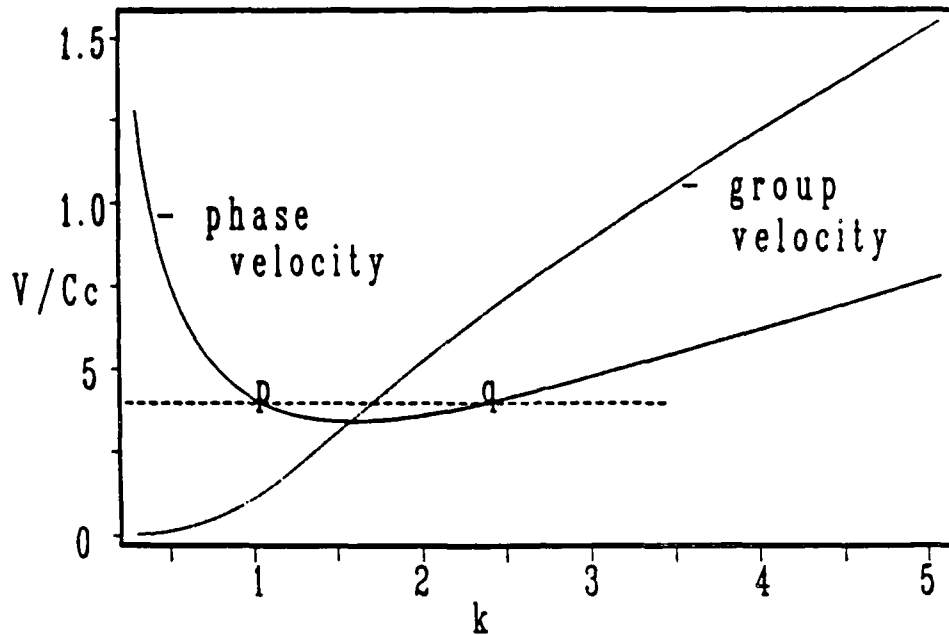

Figure 2. Phase and group velocities--thin shell theory.

For the purpose of discussion, it can be considered axiomatic that if waves are generated by a moving axisymmetric pressure Q, the phase velocity of these waves will be the velocity of this moving pressure. That is, the load must be in phase with the wave(s) it creates. With this in mind, Figure 2 shows that such waves are possible provided the load velocity equals or exceeds the minimum possible value. Let us assume for the moment that the load velocity (the projectile velocity) somewhat exceeds this minimum. According to Figure 2, there are two waves with this phase velocity. Now, physically we know that the energy contained in these two waves must radiate away, not toward, the source of the disturbance, namely the moving pressure front. Further, it is known that energy travels not at the phase velocity, but at another velocity called the 'group velocity,' related to the phase velocity as follows:

$$v_g(k) = k \frac{dv(k)}{dk} + v(k) \tag{3}$$

where $v(k)$ is the phase velocity (dispersion curve) from Figure 2. A plot of group velocity versus wave number is also shown in Figure 2 and provides a criterion for deciding whether a given wave belongs in the region $\xi > 0$ or $\xi < 0$. For example, the wave corresponding to the point p has a group velocity which is smaller than its phase velocity. Since the wave energy must flow away, not toward, the pressure front at $\xi = 0$, this wave belongs in the region $\xi < 0$ only, i.e., it is a 'trailing wave.' Conversely, the wave corresponding to the point q is a 'head wave,' belonging to the region $\xi > 0$. Assigning the two waves to their appropriate regions results in the following solution for the midwall displacement $w(x,t)$ when the load velocity v is greater than the minimum phase velocity of Figure 2

$$\frac{w^{(1)}}{C} = \frac{-b^2}{b^2 - a^2} \cos a\xi + 1 \quad ; \quad \xi \leqslant 0$$
$$\frac{w^{(2)}}{C} = \frac{-a^2}{b^2 - a^2} \cos b\xi \quad ; \quad \xi \geqslant 0 \tag{4}$$

where

$$a = \sqrt{\frac{1 + \lambda}{2}} - \sqrt{\frac{\lambda - 1}{2}} \quad ; \quad b = \sqrt{\frac{1 + \lambda}{2}} + \sqrt{\frac{\lambda - 1}{2}} \quad ; \quad \lambda = \frac{mv^2}{2} \sqrt{\frac{R^2}{EhD}}$$

and $C = QR^2/Eh$ approximates the Lamé displacement. Note that for $\lambda \gg 1$, the solution for $x \leqslant vt$ approaches 2C, twice the Lamé displacement.

It can easily be seen from Eq. (3) that should dv/dk ever vanish, the group velocity and the phase velocity would be equal and energy could not radiate away from the pressure front, but would continually build the deformation in the neighborhood of the front as time progressed, i.e., resonance would result. Thus, the minimum phase velocity of Figure 2 is indeed a 'critical velocity' and it is the near attainment of this velocity which caused the high strains in the 120-mm gun tube.

Finally, if the velocity of the moving pressure is less than the minimum possible for wave formation, the wave number k is complex and the solution to Eq. (1) has the form of a damped harmonic

$$\frac{w^{(1)}}{c} = \frac{e^{d\xi}}{2} \left(-\cos c\xi + \frac{d^2 - c^2}{2cd} \sin c\xi \right) + 1 \quad ; \quad \xi \leq 0$$

$$\frac{w^{(2)}}{c} = \frac{e^{-d\xi}}{2} \left(\cos c\xi + \frac{d^2 - c^2}{2cd} \sin c\xi \right) \quad ; \quad \xi \leq 0$$

(5)

where

$$c = \sqrt{\frac{\lambda + 1}{2}} \quad \text{and} \quad d = \sqrt{\frac{1 - \lambda}{2}}$$

A REFINED MODEL FOR THE 120-MM GUN TUBE

From the standpoint of gun tube design, it is important to be able to predict critical velocities as accurately as possible and to be able to predict the steady-state deformation at any velocity of the pressure front. Thus, it is necessary to use a model which is not restricted to cylinders with thin walls. Axisymmetric equations of motion for thick-walled cylinders have been derived by Mirsky and Herrmann (ref 5) and are considerably more complicated than Eq. (1). They are used to obtain the results which follow in much the same way as discussed previously. These equations and the details leading to their solution have been reported by the author (ref 6).

Although transient effects, boundary reflections, non-uniformity of wall thickness, and variable pressure (projectile) velocity are ignored, steady-state calculations for thick-walled cylinders nevertheless produce results in remarkable agreement with measured values when the projectile velocity is close to critical. (The assumption of constant projectile velocity is justified in the forward regions of many gun tubes where the projectile velocity/travel curve is relatively flat.) Figures 3 and 4 compare predicted and measured values of
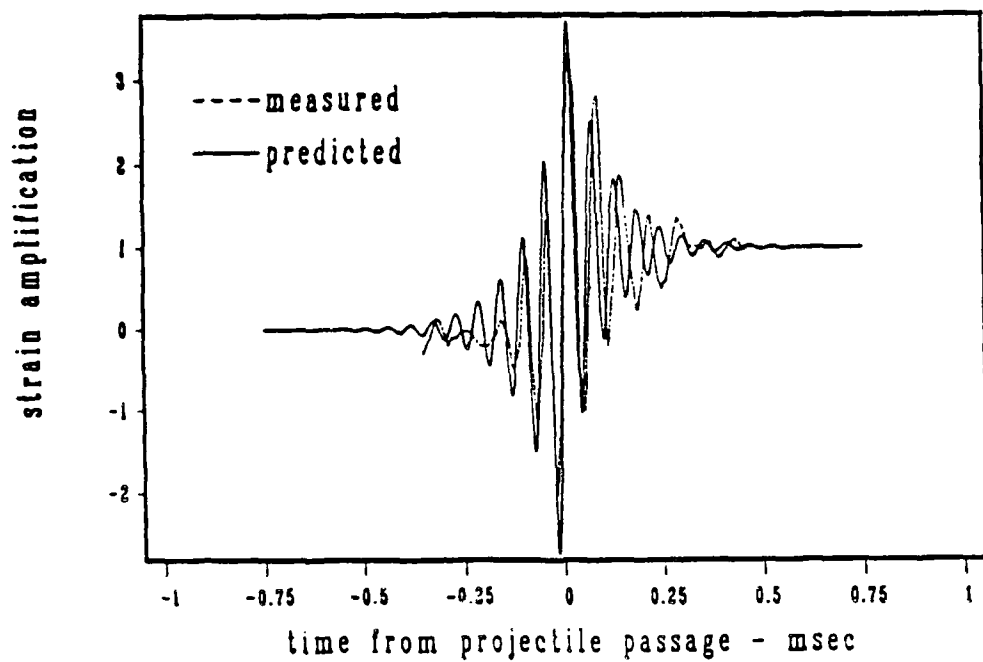
6

Figure 3.   Comparison of measured and predicted circumferential strains
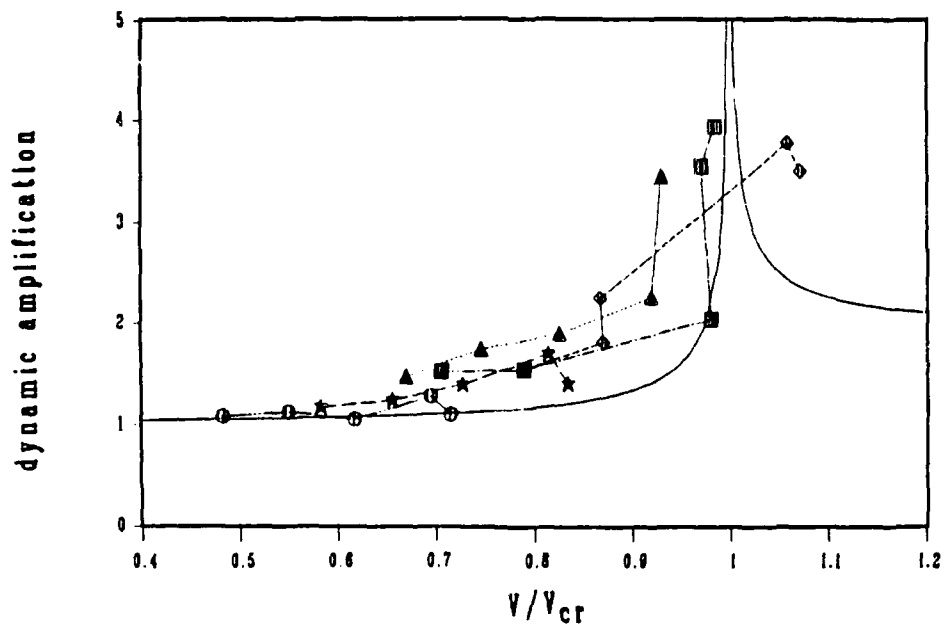located at the pressure front.

Figure 4.   Comparison of measured and predicted circumferential strains
located at the pressure front.

7

circumferential strain. Figure 3 shows the tube deformation in the neighborhood of the projectile and Figure 4 shows the maximum strain as a function of projectile velocity. The strains have been normalized with respect to the static values predicted by the Lamé formula. The disagreement between the measured and predicted strains at low velocities may be partly due to transient deformation and non-axially symmetric deformation induced through coupling. Neither of these is accounted for in the preceding axisymmetric steady-state theory. The latter is the main subject of this report.

AXISYMMETRIC AND NON-AXIALLY SYMMETRIC WAVE COUPLING

In addition to the axisymmetric equations mentioned in the last section, Mirsky and Herrmann (ref 7) have also derived a set of five equations governing both axisymmetric and non-axially symmetric motions of a uniform hollow cylinder. Gazis (ref 8) has gone a step further, accomplishing the same using the more accurate three-dimensional equations of elasticity. These investigators have computed the dispersion curves for several of these modes. Viewed in the context of critical velocity theory, it is interesting that the dispersion curves of the first non-axially symmetric mode and the previously considered axisymmetric mode have minimum values in close proximity to one another. This is shown in Figure 5. Both curves were constructed using the equations of Mirsky and Herrmann. The ordinate values have been normalized with respect to the velocity of shear waves in the material, $C_s = \sqrt{G/\rho}$, where G is the shear modulus of the material. The abscissa is the non-dimensional wave number h/L, where L is the wave length. The non-axially symmetric mode referred to in the figure corresponds to a beamlike deformation of the axis of the cylinder. Since the moving pressure is perfectly axisymmetric, the only means for exciting real waves of this type, in particular the resonance indicated by the minimum, is by

8

some sort of coupling whereby energy can be exchanged between the axisymmetric and non-axially symmetric modes.
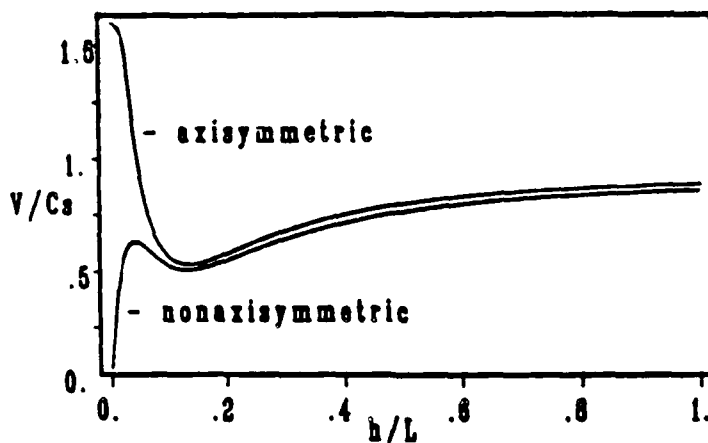

Figure 5.   Uncoupled dispersion curves (ϵ = 0)--Mirsky and Herrmann, thick-wall shell theory.

One source of modal coupling which is of importance in gun tube design is the non-uniformity of the thickness of the tube wall. Intuitively, it is clear that when a tube having an eccentric wall thickness is dynamically pressurized, the bore centerline tends to move as well as the tube wall. In effect, the eccentricity of the wall thickness creates a non-axially symmetric wall stiffness and inertia. A good indication of what may be expected has been obtained by neglecting the asymmetric stiffness and including only the eccentric inertia coupling. This is the work reported herein.

Basically, it is assumed that we are dealing with a cylinder which has a sinusoidal distribution of mass around its circumference and that this distribution is uniform along the direction of the bore axis. Thus

$$\rho = \rho_0(1 + \epsilon \cos \theta) \tag{6}$$

represents the mass distribution of the cylinder with ϵ serving as the eccentricity parameter. ρ_0 is the mass density of the material. The coupling effect sought does not require the use of sophisticated thick-wall cylinder equations

9

such as those used by Mirsky and Herrmann or those employed by Gazis, and considering the idealism reflected in neglecting asymmetric stiffness effects and the assumed mass distribution of Eq. (6) above, the use of such equations is not required. However, the essential character of the dispersion curves--especially near the dual minimums and throughout the long wave regions--must be contained in whatever equations are chosen. It is surprising that the Donnell-Mushtari equations (ref 9) do not suffice for this purpose, failing to provide a dispersion curve for the beamlike vibration which passes through the origin. Consequently, the equations of Flugge were chosen. Though more complicated than those of Donnell-Mushtari, these equations provide the necessary features in the dispersion curves and are considerably simpler than those of Mirsky and Herrmann.

The Flugge equations of motion are as follows (ref 9):

$$\left[\begin{array}{ccc} \left[\dfrac{\partial^2}{\partial s^2} + \dfrac{(1-\nu)}{2}\dfrac{\partial^2}{\partial\theta^2} - \rho\dfrac{(1-\nu^2)R^2}{E}\dfrac{\partial^2}{\partial t^2}\right] & \dfrac{(1+\nu)}{2}\dfrac{\partial^2}{\partial s\partial\theta} & \nu\dfrac{\partial}{\partial s} \\[2em] \dfrac{(1+\nu)}{2}\dfrac{\partial^2}{\partial s\partial\theta} & \left[\dfrac{(1-\nu)}{2}\dfrac{\partial^2}{\partial s^2} + \dfrac{\partial^2}{\partial\theta^2} - \rho\dfrac{(1-\nu^2)R^2}{E}\dfrac{\partial^2}{\partial t^2}\right] & \dfrac{\partial}{\partial\theta} \\[2em] \nu\dfrac{\partial}{\partial s} & \dfrac{\partial}{\partial\theta} & 1+k\nabla^4+\rho\dfrac{(1-\nu^2)R^2}{E}\dfrac{\partial^2}{\partial t^2} \end{array} \right] +$$

$$
k \begin{bmatrix}
\dfrac{(1-\nu)}{2}\dfrac{\partial^2}{\partial\theta^2} & 0 & -\dfrac{\partial^3}{\partial s^3} + \dfrac{(1-\nu)}{2}\dfrac{\partial^3}{\partial s\partial\theta^2} \\[2em]
0 & \dfrac{3(1-\nu)}{2}\dfrac{\partial^2}{\partial s^2} & -\dfrac{(3-\nu)}{2}\dfrac{\partial^3}{\partial s^2\partial\theta} \\[2em]
-\dfrac{\partial^3}{\partial s^3} + \dfrac{(1-\nu)}{2}\dfrac{\partial^3}{\partial s\partial\theta^2} & -\dfrac{(3-\nu)}{2}\dfrac{\partial^3}{\partial s^2\partial\theta} & 1 + 2\dfrac{\partial^2}{\partial\theta^2}
\end{bmatrix}
\begin{bmatrix} u \\[2em] v \\[2em] w \end{bmatrix}
=
\begin{bmatrix} 0 \\[2em] 0 \\[2em] Q \end{bmatrix}
\tag{7}
$$

where $k = h^2/12R^2$, $s = x/R$, and θ is measured tangentially. u, v, and w are the displacement components in the x, θ, and R directions, respectively. $Q = pR^2(1-\nu^2)/Eh$ is the applied load due to the pressure p.

Solutions to Eq. (7) are assumed in the form of a linear superposition of axisymmetric motion (u_0, w_0) and motion from the first non-axially symmetric mode (u_1, v_1, w_1). (v_0 can be omitted because it produces an equation for torsional motion which is uncoupled from the non-axially symmetric variables.) Thus,

$$u(s,\theta,t) = u_0(x,t) + u_1(x,t)\cos\theta$$

$$v(s,\theta,t) = v_1(x,t)\sin\theta$$

$$w(s,\theta,t) = w_0(x,t) + w_1(x,t)\cos\theta \tag{8}$$

Equations (8) can be considered as approximation functions for use with the Galerkin method (ref 10). The variations $\delta u = \delta u_0 + \delta u_1 \cos\theta$, $\delta v = \delta v_1 \sin\theta$, and $\delta w = \delta w_0 + \delta w_1 \cos\theta$ multiply the first, second, and third of Eqs. (8), respectively. The resulting expressions and Eq. (6) for $\rho(\theta)$ are substituted in Eq. (7) followed by an integration between the limits $\theta = 0$ and 2π. This results in the five equations:

$$-k\frac{\partial^3 w_0}{\partial s^3} + \nu\frac{\partial w_0}{\partial s} - \frac{\epsilon}{2}\frac{\partial^2 u_1}{\partial t^2} - \frac{\partial^2 u_0}{\partial t^2} + \frac{\partial^2 u_0}{\partial s^2} = 0$$

$$-k\frac{\partial^3 w_1}{\partial s^3} + \nu\frac{\partial w_1}{\partial s} - \frac{k}{2}(1-\nu)\frac{\partial w_1}{\partial s} + \frac{(\nu+1)}{2}\frac{\partial v_1}{\partial s} - \frac{\partial^2 u_1}{\partial t^2} + \frac{\partial^2 u_1}{\partial s^2}$$

$$-k\frac{(1-\nu)}{2}u_1 - \frac{(1-\nu)}{2}u_1 - \epsilon\frac{\partial^2 u_0}{\partial t^2} = 0$$

$$\frac{k}{2}(3-\nu)\frac{\partial^2 w_1}{\partial s^2} - w_1 - \frac{\partial^2 v_1}{\partial t^2} + \frac{3k(1-\nu)}{2}\frac{\partial^2 v_1}{\partial s^2} + \frac{(1-\nu)}{2}\frac{\partial^2 v_1}{\partial s^2} - v_1 - \frac{(\nu+1)}{2}\frac{\partial u_1}{\partial s} = 0$$

$$\frac{\epsilon}{2}\frac{\partial^2 w_1}{\partial t^2} + \frac{\partial^2 w_0}{\partial t^2} + k\frac{\partial^4 w_0}{\partial s^4} + kw_0 + w_0 - k\frac{\partial^3 u_0}{\partial s^3} + \nu\frac{\partial u_0}{\partial s} = Q$$

$$\frac{\partial^2 w_0}{\partial t^2} + k\frac{\partial^4 w_1}{\partial s^4} - 2k\frac{\partial^2 w_1}{\partial s^2} + w_1 + \epsilon\frac{\partial^2 w_0}{\partial t^2} - k\frac{(3-\nu)}{2}\frac{\partial^2 v_1}{\partial s^2} + v_1$$

$$-k\frac{\partial^3 u_1}{\partial s^3} + \nu\frac{\partial u_1}{\partial s} - \frac{k(1-\nu)}{2}\frac{\partial u_1}{\partial s} = 0 \tag{9}$$

Steady-state solutions to Eqs. (9) can be obtained in exactly the same way as the steady-state solution to Eq. (1). Under the substitution $\xi = s - v\tau$ (where $\tau = [E/\rho_0 R^2(1-\nu^2)]^{\frac{1}{2}}t$), Eqs. (9) become five ordinary differential equations with ξ as the independent variable.

$$-kw_0''' + \nu w_0' - \frac{\epsilon v^2}{2}u_1'' + (1-v^2)u_0'' = 0$$

$$-2kw_1''' + [\nu(k+2) - k]w_1' (1+\nu)v_1' + 2(1-v^2)u_1'' - 2\epsilon v^2 u_0''$$

$$+ [(k+1)(\nu-1)]u_1 = 0$$

$$k(3-\nu)w_1'' - 2w_1 - [2v^2 + (3k+1)(\nu-1)]v_1'' - 2v_1 - (1+\nu)u_1' = 0$$

$$\frac{\epsilon v^2}{2}w_1'' + kw_0'''' + v^2 w_0'' + (k+1)w_0 - ku_0''' + \nu u_0' = Q$$

$$kw_1'''' + (v^2-2k)w_1'' + w_1 + \epsilon v^2 w_0'' + \frac{k}{2}(\nu-3)v_1'' + v_1 - ku_1'''$$

$$+ [\frac{k}{2}(\nu-1) + \nu]u_1' = 0 \tag{10}$$

The complementary solutions of Eqs. (10) are obtained by substituting solutions of the form $A_j e^{-i\alpha\xi}$ for each of the variables u_0, u_1, v_1, w_0, and w_1, where A_j is a different arbitrary constant in each substitution and α is the wave number. The result is a set of five linear equations which only have non-trivial solutions if the determinant of the coefficients of the A_j vanishes, i.e.,

$\alpha^2(v^2-1)$	$\dfrac{\alpha^2\epsilon v^2}{2}$	0	$-i\alpha(v+\alpha^2 k)$	0
$\alpha^2\epsilon v^2$	$\alpha^2(v^2-1) + \dfrac{v}{2}(k+1) - \dfrac{1}{2}(k+1)$	$-\dfrac{i\alpha}{2}(1+v)$	0	$-i\alpha(\dfrac{kv}{2}+v+\alpha^2 k - \dfrac{k}{2})$
0	$\dfrac{i\alpha}{2}(1+v)$	$\dfrac{\alpha^2}{2}[2v^2+v(3k+1)-3k-1]-1$	0	$\dfrac{\alpha^2 k}{2}(v-3)-1$
$-i\alpha(v+\alpha^2 k)$	0	0	$-\alpha^2(v^2-\alpha^2 k)+k+1$	$-\dfrac{\alpha^2\epsilon v^2}{2}$
0	$-i\alpha(\dfrac{kv}{2}+v+\alpha^2 k - \dfrac{k}{2})$	$\dfrac{\alpha^2 k}{2}(3-v)+1$	$-\alpha^2\epsilon v^2$	$-\alpha^2(v^2-\alpha^2 k-2k)+1$

(11)

Setting this determinant to zero results in the dispersion relation. The first two branches are shown in Figure 6 for the value $\epsilon = 0.1$. The similarity to those of Mirsky and Herrmann (Figure 5) is evident.

The dispersion curves of Figure 6 represent the natural (unforced) waves of the cylinder which are the complementary solutions to Eq. (10). As was the case in dealing with Eq. (1), the stresses and displacements are required to be continuous at the location of the pressure front. In terms of the variables

13

defined in Eqs. (8), the following quantities must be continuous at $\xi = 0$ (ref 11):

$$\frac{h^2}{4R^2}(w_1' + v_1') + v_1' - u_1' \; ,$$

$$\nu(w_1 + v_1) + u_1' - w_1'' \; ,$$

$$w_0'' - u_0' \; ,$$

$$(\tfrac{\nu-1}{2})u_1 + (\nu-2)w_1' + \frac{(\nu-3)}{2} v_1' + w_1''' - u_1'' \; ,$$

$$, \; w_0''' - u_0'' \; ,$$
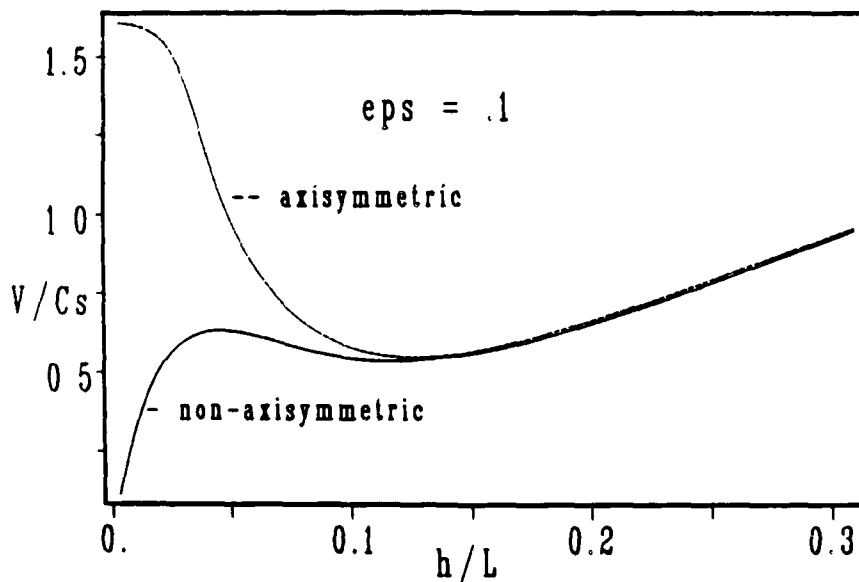
and

$$v_1, \; w_0, \; w_1, \; w_0', \; w_1'$$

Figure 6. Coupled dispersion curves ($\epsilon = 0.1$) using shell theory of Flugge.

The continuity relations plus the boundedness criteria at infinity and/or the group velocity argument are sufficient to uniquely determine the displacements once the particular solutions have been determined. The particular solutions corresponding to the load terms on the right-hand side of Eqs. (9) may be found by eliminating all but one of the dependent variables through the use of

Cramer's rule and the commutativity of the differential operators (ref 12).

This procedure is much simpler than inverting Fourier transforms--a common solution technique used in connection with these problems (cf. (ref 3)).

From the previous discussion in connection with Eq. (1), several load velocities are of interest. For example, from the dispersion curves of Figure 6, it is clear that a real wave will be excited regardless of how small the projectile velocity might be. As a typical value, $v = 0.382 \, C_S$ has been chosen and the corresponding mid-wall radial displacement at the top of the cylinder ($\theta = 0$) is shown in Figure 7 using the value $\epsilon = 0.1$ (10 percent mass eccentricity).
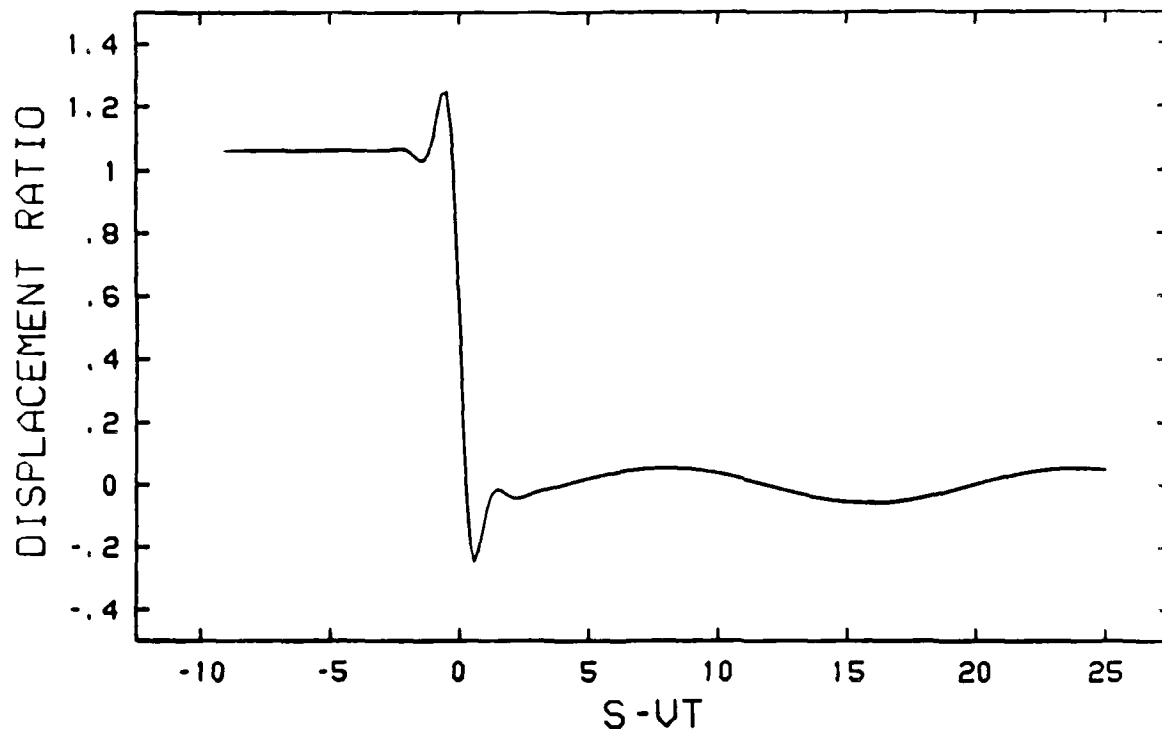

Figure 7. Radial displacement from coupled Flugge equations,
$v/C_S = 0.382$, $\epsilon = 0.1$.

The ordinate in Figures 7 through 10 is the ratio of the dynamic displacement in the radial direction (w) to the static axisymmetric radial displacement as approximated by the particular solution for w_0. This radial displacement is essentially quasi-static except for the existence of a wave which, from the

15

group velocity argument, exists in front of the pressure only. The presence of any 'head wave' will be felt at the gun muzzle prior to the arrival of the projectile and therefore constitutes a possible cause of round inaccuracy at the target.

Another load velocity of interest is $v = 0.515\ C_S$ which is just below the lowest critical value. Again, $\epsilon = 0.1$ and the radial displacement at the top of the cylinder is shown in Figure 8a. The head wave of Figure 7 is evident. The axisymmetric portion of this displacement is shown in Figure 8b, so that the difference between the two figures is the contribution of the beamlike motion at this velocity and is substantial.
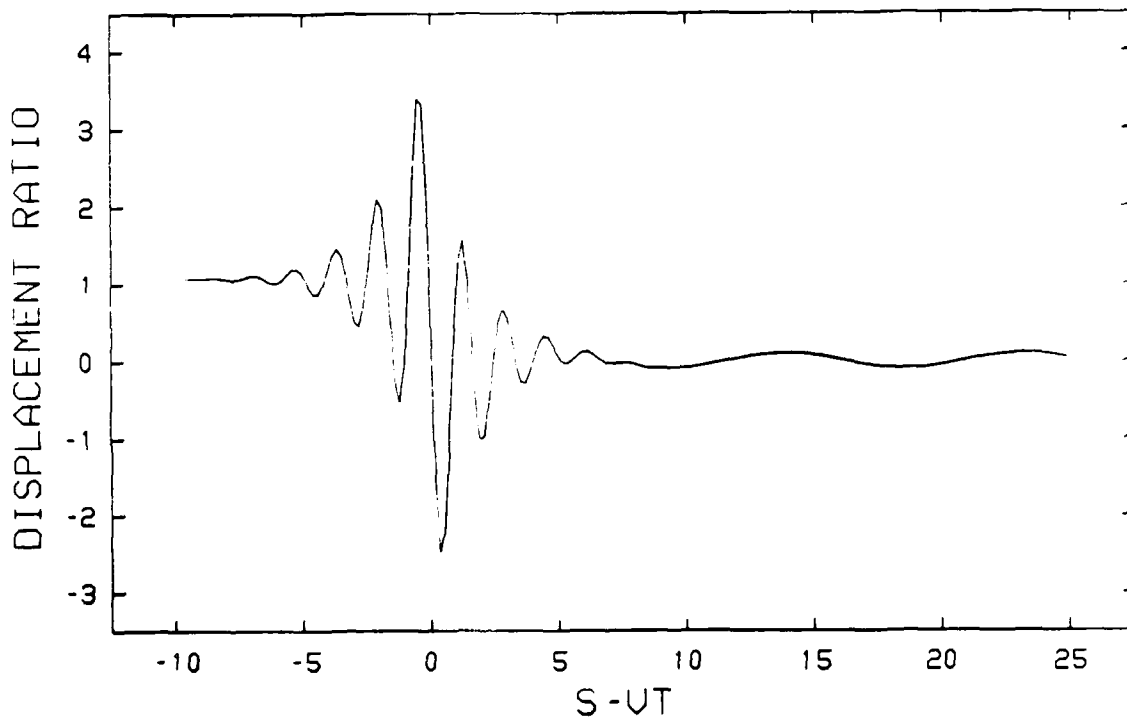

Figure 8a. Radial displacement, $\theta = 0$, $v/C_S = 0.515$, $\epsilon = 0.1$.
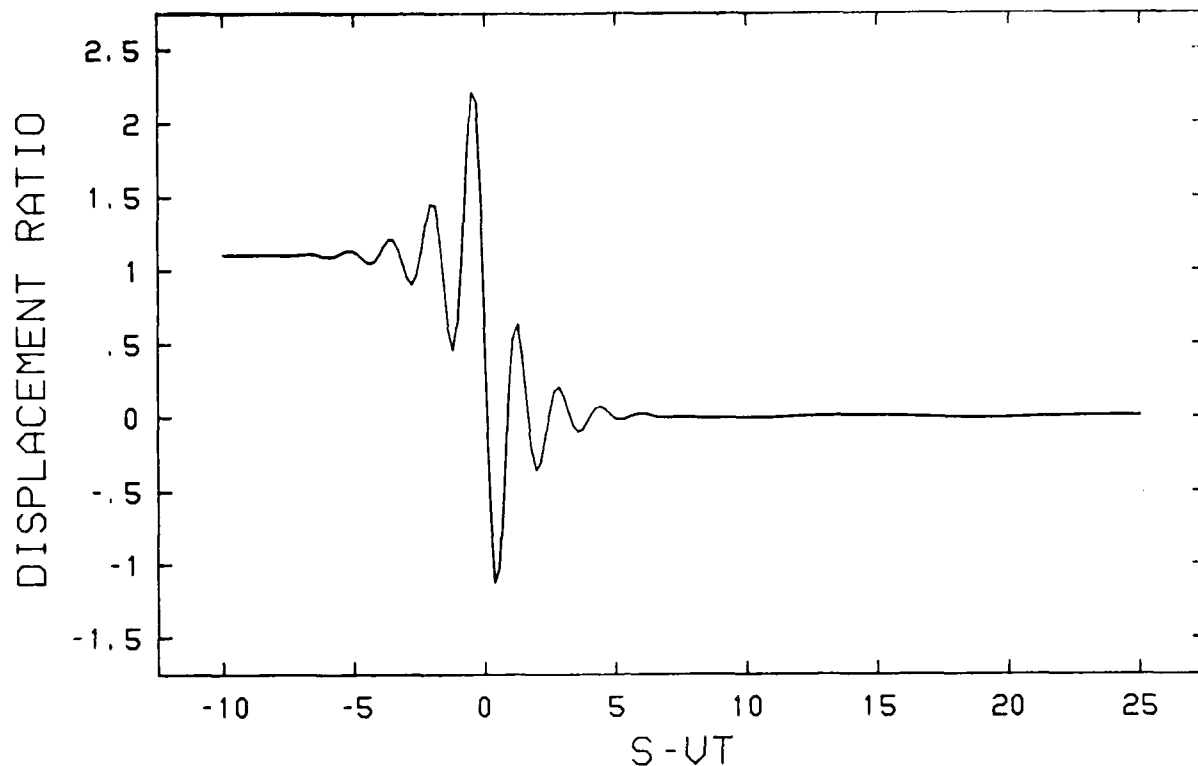
Figure 8b. Axisymmetric component of Figure 8a.

The presence of a maximum value in the long wavelength region of the lower dispersion curve is also cause for interest. It is known, however, that the dispersion curve for the next non-axially symmetric mode (in which the tube distorts more or less into an elliptical shape) passes through this region and has a minimum value there. This mode is not included in the present analysis and therefore the model is considered to be inaccurate in this region.

Probably the most interesting load velocity is that which falls between the minimums (V_{cr1}, V_{cr2}) of the two curves of Figure 6. For a load velocity exactly halfway between these minimums, i.e.,

$$V = \frac{V_{cr1} + V_{cr2}}{2}$$

Figure 9 shows that the axisymmetric and beamlike motions are nearly equal in magnitude for values of ϵ as small as 0.01. This is apparently due to the fact that the minimums (critical velocities) of the two branches of Figure 6 approach each other as ϵ diminishes. Consequently, a load velocity halfway between them is closer to both critical values when ϵ is smaller. This is shown in Figure 10--a blowup of Figure 6 in the vicinity of the minimums in the neighborhood of the critical velocities for two values of ϵ. From one point of view, the non-axially symmetric wave acts as a vibration absorber for the axisymmetric motion. This is not likely to reduce the maximum stress in the cylinder, however, since the wall will then be subjected to biaxial stresses of comparable magnitudes.
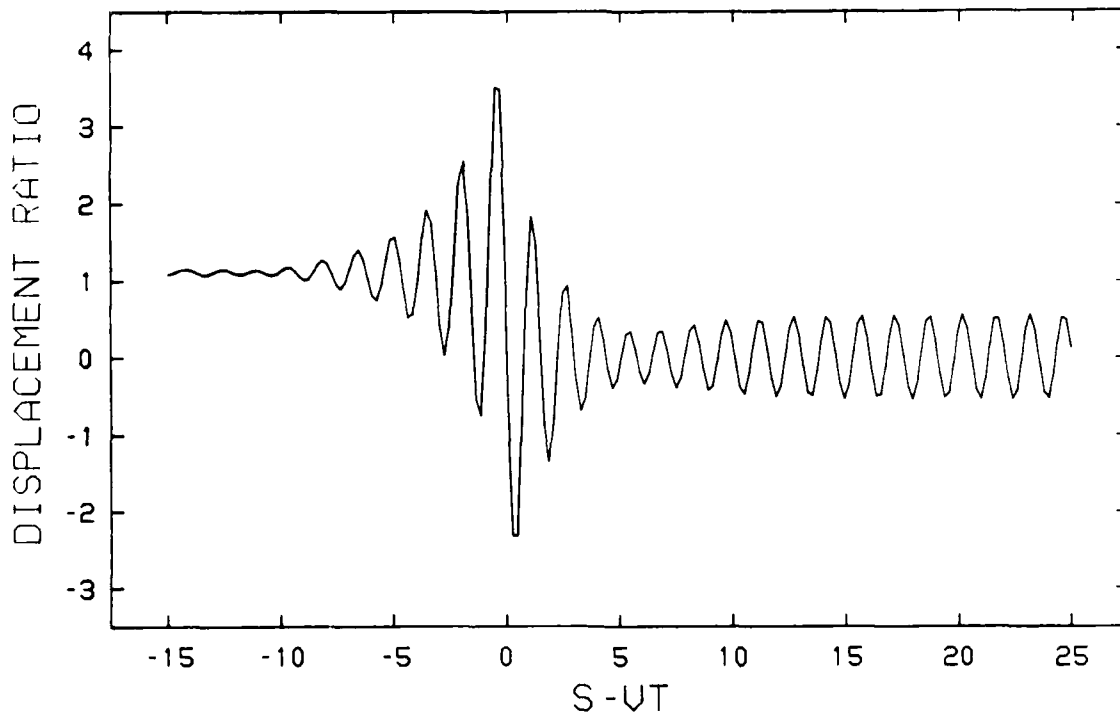

Figure 9a. Axisymmetric component of radial displacement, $\theta = 0$,

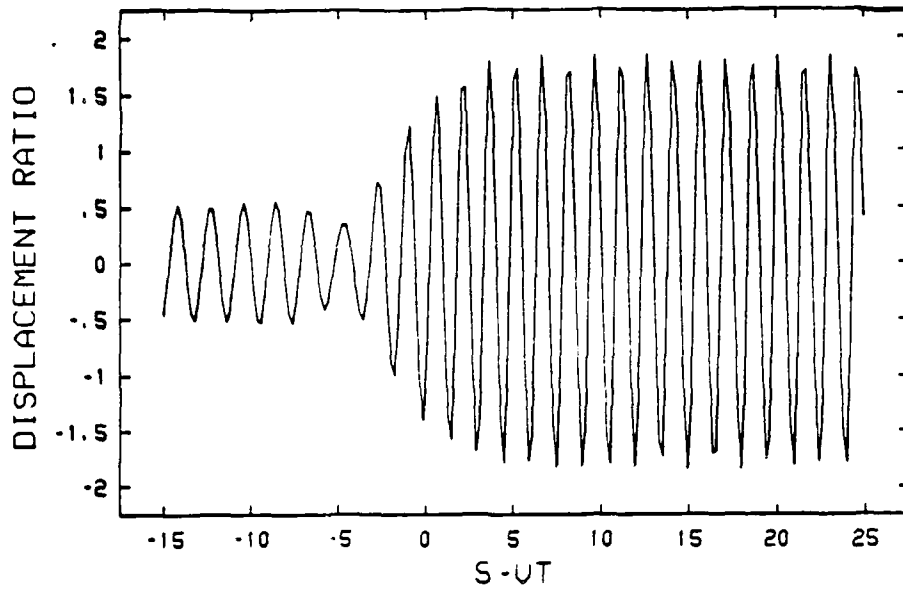$$v = \frac{V_{cr1} + V_{cr2}}{2} = 0.541, \ \epsilon = 0.01.$$

Figure 9b. Non-axially symmetric (beamlike) component of radial displacement. $\theta = 0$,

$$v = \frac{V_{cr1} + V_{cr2}}{2} = 0.541, \; \epsilon = 0.01.$$
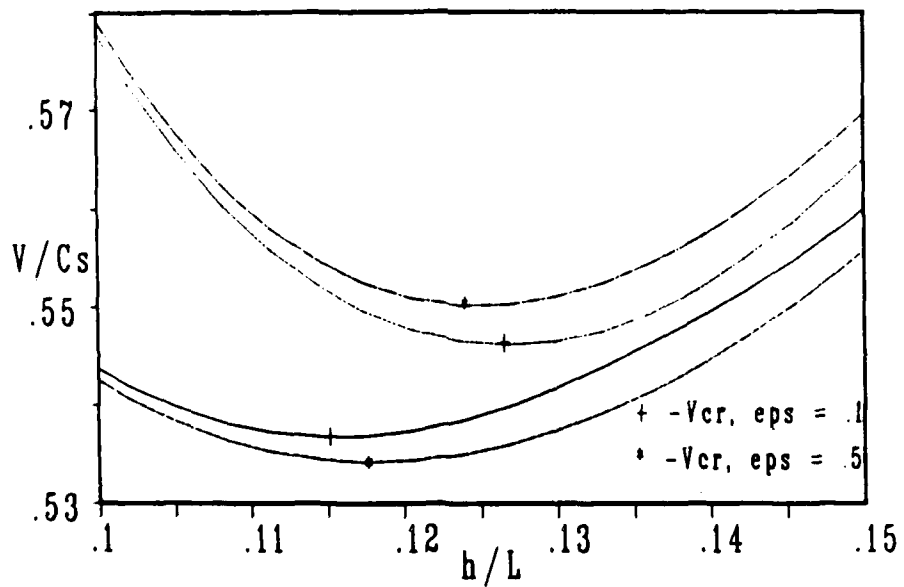

Figure 10. Dispersion curves near their minimum values, $\epsilon = 0.1$ and $\epsilon = 0.5$.

REFERENCES

1. S. P. Timoshenko and J. N. Goodier, _Theory of Elasticity_, Third Edition, McGraw-Hill, 1970, pp. 68-71.

2. H. Reismann, "Response of a Prestressed Cylindrical Shell to Moving Pressure Load, Developments in Mechanics," in: _Solid Mechanics - Proceedings of the Eighth Midwestern Mechanics Conference_, Pergamon Press, Part II, Vol. 2, 1965, pp. 349-363.

3. S. Tang, "Dynamic Response of a Tube Under Moving Pressure," _Journal of the Engineering Mechanics Division_, _Proceedings of the ASCE_, Part 1, Vol. 91, October 1965, pp. 97-122.

4. J. P. Jones and P. G. Bhuta, "Response of Cylindrical Shells to Moving Loads," _Journal of Applied Mechanics_, Vol. 31, March 1964, pp. 105-111.

5. I. Mirsky and G. Herrmann, "Axially Symmetric Motions of Thick Cylindrical Shells," _Journal of Applied Mechanics_, Vol. 25, March 1958, pp. 97-102.

6. T. E. Simkins, "Resonance of Flexural Waves in Gun Tubes," Technical Report ARCCB-TR-87008, Benet Weapons Laboratory, Watervliet, NY, July 1987.

7. I. Mirsky and G. Herrmann, "Nonaxially Symmetric Motions of Cylindrical Shells," _Journal of the Acoustical Society of America_, Vol. 29, No. 10, October 1957, pp. 1116-1123.

8. D. C. Gazis, "Three-Dimensional Investigation of the Propagation of Waves in Hollow Cylinders: I. Analytical Foundation, II. Numerical Results," _Journal of the Acoustical Society of America_, Vol. 31, No. 5, May 1959, pp. 569-578.

9. A. W. Leissa, "Vibration of Shells," NASA SP-288, Washington, D.C., 1973, pp. 32-34.

10. L. V. Kantorovich and V. I. Krylov, _Approximate Methods of Higher Analysis_, Interscience Pubishers, New York, 1964, p. 258.

11. A. W. Leissa, "Vibration of Shells," NASA SP-288, Washington, D.C., 1973, p. 29.

12. F. B. Hildebrand, _Advanced Calculus for Engineers_, Ninth Edition, Prentice-Hall, 1960, pp. 21-22.

TECHNICAL REPORT INTERNAL DISTRIBUTION LIST

	NO. OF COPIES
CHIEF, DEVELOPMENT ENGINEERING DIVISION	
ATTN: SMCAR-CCB-D	1
-DA	1
-DC	1
-DM	1
-DP	1
-DR	1
-DS (SYSTEMS)	1
CHIEF, ENGINEERING SUPPORT DIVISION	
ATTN: SMCAR-CCB-S	1
-SE	1
CHIEF, RESEARCH DIVISION	
ATTN: SMCAR-CCB-R	2
-RA	1
-RM	1
-RP	1
-RT	1
TECHNICAL LIBRARY	5
ATTN: SMCAR-CCB-TL	
TECHNICAL PUBLICATIONS & EDITING SECTION	3
ATTN: SMCAR-CCB-TL	
DIRECTOR, OPERATIONS DIRECTORATE	1
ATTN: SMCWV-OD	
DIRECTOR, PROCUREMENT DIRECTORATE	1
ATTN: SMCWV-PP	
DIRECTOR, PRODUCT ASSURANCE DIRECTORATE	1
ATTN: SMCWV-QA	

NOTE: PLEASE NOTIFY DIRECTOR, BENET LABORATORIES, ATTN: SMCAR-CCB-TL, OF ANY ADDRESS CHANGES.

TECHNICAL REPORT EXTERNAL DISTRIBUTION LIST

	NO. OF COPIES		NO. OF COPIES
ASST SEC OF THE ARMY RESEARCH AND DEVELOPMENT ATTN: DEPT FOR SCI AND TECH THE PENTAGON WASHINGTON, D.C. 20310-0103	1	COMMANDER ROCK ISLAND ARSENAL ATTN: SMCRI-ENM ROCK ISLAND, IL 61299-5000	1
ADMINISTRATOR DEFENSE TECHNICAL INFO CENTER ATTN: DTIC-FDAC CAMERON STATION ALEXANDRIA, VA 22304-6145	12	DIRECTOR US ARMY INDUSTRIAL BASE ENGR ACTV ATTN: AMXIB-P ROCK ISLAND, IL 61299-7260	1
COMMANDER US ARMY ARDEC		COMMANDER US ARMY TANK-AUTMV R&D COMMAND ATTN: AMSTA-DDL (TECH LIB) WARREN, MI 48397-5000	1

ATTN: SMCAR-AEE
    SMCAR-AES, BLDG. 321
    SMCAR-AET-O, BLDG. 351N
    SMCAR-CC
    SMCAR-CCP-A
    SMCAR-FSA
    SMCAR-FSM-E
    SMCAR-FSS-D, BLDG. 94
    SMCAR-IMI-I (STINFO) BLDG. 59
PICATINNY ARSENAL, NJ 07806-5000
	1
	1
	1
	1
	1
	1
	1
	1
	2
		COMMANDER
		US MILITARY ACADEMY
		ATTN: DEPARTMENT OF MECHANICS
		WEST POINT, NY 10996-1792
		
		US ARMY MISSILE COMMAND
		REDSTONE SCIENTIFIC INFO CTR
		ATTN: DOCUMENTS SECT, BLDG. 4484
		REDSTONE ARSENAL, AL 35898-5241
			1
			
			2

DIRECTOR US ARMY BALLISTIC RESEARCH LABORATORY ATTN: SLCBR-DD-T, BLDG. 305 ABERDEEN PROVING GROUND, MD 21005-5066	1	COMMANDER US ARMY FGN SCIENCE AND TECH CTR ATTN: DRXST-SD 220 7TH STREET, N.E. CHARLOTTESVILLE, VA 22901	1
DIRECTOR US ARMY MATERIEL SYSTEMS ANALYSIS ACTV ATTN: AMXSY-MP ABERDEEN PROVING GROUND, MD 21005-5071	1	COMMANDER US ARMY LABCOM MATERIALS TECHNOLOGY LAB ATTN: SLCMT-IML (TECH LIB) WATERTOWN, MA 02172-0001	2
COMMANDER HQ, AMCCOM ATTN: AMSMC-IMP-L ROCK ISLAND, IL 61299-6000	1		

NOTE: PLEASE NOTIFY COMMANDER, ARMAMENT RESEARCH, DEVELOPMENT, AND ENGINEERING
CENTER, US ARMY AMCCOM, ATTN: BENET LABORATORIES, SMCAR-CCB-TL,
WATERVLIET, NY 12189-4050, OF ANY ADDRESS CHANGES.

	NO. OF COPIES		NO. OF COPIES
COMMANDER US ARMY LABCOM, ISA ATTN: SLCIS-IM-TL 2800 POWDER MILL ROAD ADELPHI, MD 20783-1145	1	COMMANDER AIR FORCE ARMAMENT LABORATORY ATTN: AFATL/MN EGLIN AFB, FL 32542-5434	1
COMMANDER US ARMY RESEARCH OFFICE ATTN: CHIEF, IPO P.O. BOX 12211 RESEARCH TRIANGLE PARK, NC 27709-2211	1	COMMANDER AIR FORCE ARMAMENT LABORATORY ATTN: AFATL/MNF EGLIN AFB, FL 32542-5434	1
DIRECTOR US NAVAL RESEARCH LAB ATTN: MATERIALS SCI & TECH DIVISION CODE 26-27 (DOC LIB) WASHINGTON, D.C. 20375	1 1	METALS AND CERAMICS INFO CTR BATTELLE COLUMBUS DIVISION 505 KING AVENUE COLUMBUS, OH 43201-2693	1

NOTE: PLEASE NOTIFY COMMANDER, ARMAMENT RESEARCH, DEVELOPMENT, AND ENGINEERING
        CENTER, US ARMY AMCCOM, ATTN: BENET LABORATORIES, SMCAR-CCB-TL,
        WATERVLIET, NY 12189-4050, OF ANY ADDRESS CHANGES.